A Letters Journal Exploring the Frontiers of Physics

December 2012

EPL, **100** (2012) 67008
doi: 10.1209/0295-5075/100/67008

www.epljournal.org

The fractional quantum Hall effect of tachyons in a topological insulator junction

Vadim M. Apalkov[1] and Tapash Chakraborty[2(a)]

[1] *Department of Physics and Astronomy, Georgia State University - Atlanta, GA 30303, USA*
[2] *Department of Physics and Astronomy, University of Manitoba - Winnipeg, Canada R3T 2N2*

received 25 September 2012; accepted in final form 3 December 2012
published online 8 January 2013

PACS 73.20.-r – Electron states at surfaces and interfaces
PACS 73.43.-f – Quantum Hall effects
PACS 03.30.+p – Special relativity

Abstract – We have studied the tachyonic excitations in the junction of two topological insulators in the presence of an external magnetic field. The Landau levels, evaluated from an effective two-dimensional model for tachyons, and from the junction states of two topological insulators, show some unique properties not seen in conventional electrons systems or in graphene. The $\nu = \frac{1}{3}$ fractional quantum Hall effect has also a strong presence in the tachyon system. Experimental confirmation of these unusual magnetic properties will confirm the presence of tachyons in the system.

The surface state of recently discovered three-dimensional topological insulators [1] contains a single Dirac cone and as a result, the charge carriers on the surface are characterized as massless Dirac fermions. Some of the properties of these particles are well known from another topological system, the graphene [2]. We have shown earlier [3] that the dispersion relation of the surface excitations in a junction between two such topological insulators (TIs) show several very unique properties. Most importantly, under certain conditions these excitations exhibit tachyon-like dispersion relation [4–6] corresponding to superluminal propagation of Dirac fermions along the interface of the two TIs. In addition to the tachyonic dispersion, the junction states can also support the usual massless relativistic dispersion relation of the Dirac fermions [7]. Here we report on the properties of these tachyonic excitations in an external magnetic field. We discuss the unique nature of the Landau levels (LLs) of these tachyons and the interaction properties of tachyons in a strong magnetic field, which leads to the fractional quantum Hall effect (FQHE) of tachyons. We consider the surface states in a junction between two TIs insulators. The system of two TIs is shown schematically in fig. 1, where the flat junction surface is at $z = 0$. The junction surface states are localized in both positive and negative directions of the z axis. The two TIs, TI-1 and TI-2, have different parameters and are in direct contact with each other. This type of junction between two TIs can be realized, for example, for the same type of TI but with different orientations of crystallographic axes in regions 1 and 2.

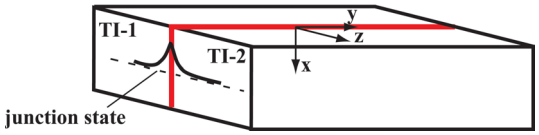

Fig. 1: (Colour on-line) A schematic view of the TI junction considered here.

Effective two-dimensional (2D) model of tachyonic excitations: The tachyons in the junction of two TIs can be described by an effective 2D matrix Hamiltonian $\mathcal{H}_{AC}$ (proposed by Apalkov and Chakraborty [3]) for Dirac fermions but with imaginary Fermi velocity (instead of the imaginary proper mass commonly attributed to the tachyons [4], *e.g.*, to the neutrinos [8])

$$\mathcal{H}_{\rm AC} = \begin{pmatrix} \Delta_0 & iv_{\rm I}p_+ \\ iv_{\rm I}p_- & -\Delta_0 \end{pmatrix} = \Delta_0\sigma_z + iv_{\rm I}(\vec{\sigma}\vec{p}), \qquad (1)$$

where $p_\pm = p_x \pm p_y$ is the 2D momentum, Δ_0 is the effective mass of the tachyons, $iv_{\rm I}$ is the imaginary Fermi velocity, and $\vec{\sigma}$ are the Pauli spin matrices. This effective

(a) E-mail: tapash@physics.umanitoba.ca

Hamiltonian has the tachyon-like dispersion, $E_{\rm Tach}(p) = \pm\sqrt{\Delta_0^2 - v_{\rm I}p^2}$, where $p = \left(p_x^2 + p_y^2\right)^{\frac{1}{2}}$. Typical values of the parameters are $\Delta_0 \sim 0.3\,$eV and $v_{\rm I} \sim 10^6$ m/s [3].

We subject the tachyon system to an external magnetic field, B, pointing along the z-direction, *i.e.*, perpendicular to the junction between the TIs. The Hamiltonian describing such a system in a magnetic field can be found from the Hamiltonian (1) upon replacing the tachyonic momentum, (p_x, p_y) by the generalized momentum, (π_x, π_y) and introducing the Zeeman energy, $\Delta_z(B) = \frac{1}{2}g_s\mu_B B$. Here μ_B is the Bohr magneton and $g_s \approx 8$ is the effective g-factor of the tachyons, which we assume to be equal to the g-factor of the TI surface states [9,10]. The tachyonic Hamiltonian is then

$$\mathcal{H}_{\rm AC}(B) = [\Delta_0 + \Delta_z(B)]\,\sigma_z + {\rm i}v_{\rm I}(\vec{\sigma}\vec{\pi}). \qquad (2)$$

The LL energy spectrum corresponding to the Hamiltonian (eq. (2)) is characterized by an integer number $n \geqslant 0$ (the LL index), and is defined as

$$\begin{aligned} E_{n=0} &= \Delta_0 + \Delta_z(B), \\ E_{n\geqslant 1,s} &= s\,[\Delta_0 + \Delta_z(B)]\,[1 - nB/B^*(B)]^{\frac{1}{2}}\,. \end{aligned} \qquad (3)$$

Here $s = \pm 1$ and we introduced the effective magnetic field $B^*(B) = \frac{e}{2\hbar c}[(\Delta_0 + \Delta_z(B))/v_{\rm I}]^2$.

The wave functions corresponding to the LLs (eq. (3)) can be expressed in terms of the functions $\phi_{n,m}$, which are wave functions of the conventional ("non-relativistic") LLs with index n and the intra-LL index, m, for example, the z component of the angular momentum. The LL wave functions of the tachyons are

$$\Psi^{\rm (Tach)}_{n=0} = \begin{pmatrix} \phi_{0,m} \\ 0 \end{pmatrix}, \quad \Psi^{\rm (Tach)}_{n\geqslant 1,s} = \begin{pmatrix} \cos\alpha_{n,s}\,\phi_{n,m} \\ \sin\alpha_{n,s}\,\phi_{n-1,m} \end{pmatrix}, \qquad (4)$$

where $\alpha_{n,s} = \arcsin[\frac{1}{2}(1 - s\sqrt{1 - nB/B^*})]^{1/2}$.

The LL energy spectrum obtained from eq. (3) is shown in fig. 2. The energy spectrum for tachyons exhibits a few distinct features: i) The LL energy spectrum is mainly restricted within the energy interval $-\Delta_0 < E_{n,s} < \Delta_0$. ii) At a given magnetic field B, only the LL with index $n < B^*/B$ can be observed. Therefore, for a given magnetic field, only a few LLs exist in the system and, for a large enough magnetic field (*e.g.*, $B > 32$ tesla in fig. 2(a)), only the $n = 0$ LL survives. This behavior of the LL of tachyonic excitations is totally different from that in conventional semiconductors with the LL energy spectrum $E_n \propto nB$, and in graphene, where $E_n \propto \sqrt{nB}$ [2]. However, there is one similarity between the tachyonic LL dispersion relations and those in graphene. In both cases there is one $n = 0$ LL, whose energy is independent of the strength of the magnetic field (without the Zeeman splitting). In graphene, the energy of this LL is $E_{n=0} = 0$, while for tachyons, $E_{n=0} = \Delta_0$. In both cases the corresponding wave functions are $\phi_{n=0,m}$. In the above analysis we assumed that the effective g-factor of tachyons is $g_s \approx 8$, which corresponds to the g-factor of the surface state of isolated TI. The variation of the g-factor changes the scale of the magnetic fields shown in fig. 3. With increasing g_s the range of magnetic fields at which the LLs can be observed, decreases. For a relatively large g-factor, the corresponding LLs cannot be realized. For example, if $g_s > 70$ then the tachyon dispersion does not have the $n = 1$ LL.

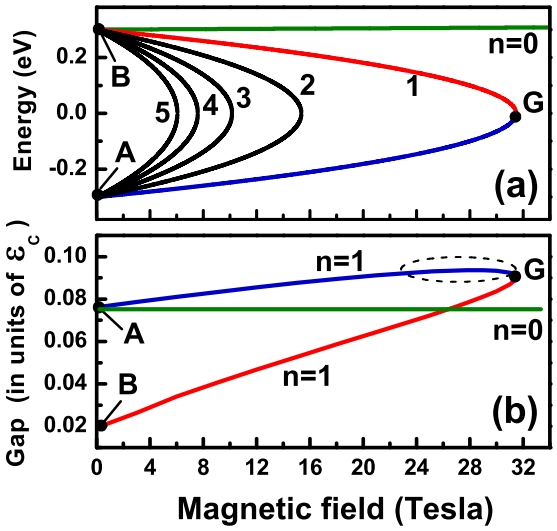

Fig. 2: (Colour on-line) (a) The LLs of the effective 2D tachyon Hamiltonian (1) are shown as a function of the magnetic field. The numbers next to the lines are the LL indices. The $n = 1$ LL wave functions at points A and B are identical to conventional "non-relativistic" LLs with indices 0 and 1, respectively. At point G, the LL wave function of the tachyon system is identical to the $n = 1$ LL wave function of graphene. (b) $\nu = \frac{1}{3}$ gap (see footnote [1]) is shown for the $n = 0$ and $n = 1$ LLs of tachyons. The gap is calculated for a finite-size system with $N = 9$ particles in a spherical geometry with parameter $S = 12$. The red and blue lines correspond to the $n = 1$ LL branches shown in panel (a). The gap is measured in units of the Coulomb energy, $\epsilon_{\rm C} = e^2/\kappa\ell_0$. The dashed curve is explained in the text.

To address the similarities and differences between the LL wave functions of the tachyon system and those of graphene (or even conventional semiconductor systems), we consider the interaction properties of tachyonic excitations in a given LL. To characterize the strength of the inter-tachyonic interactions we study the strength of the FQHE, *i.e.*, the magnitude of the gap[1]. In the FQHE regime the electrons partially occupy a single LL and the properties of such a system are characterized by the interparticle interactions within the corresponding LL [11]. The interaction strength within a given LL is determined from the Haldane pseudopotentials, V_m [12], which are the interaction energies of two particles with relative angular

[1]In what follows, by "gap" we mean the quasiparticle quasihole gap in a FQHE filling factor [11].

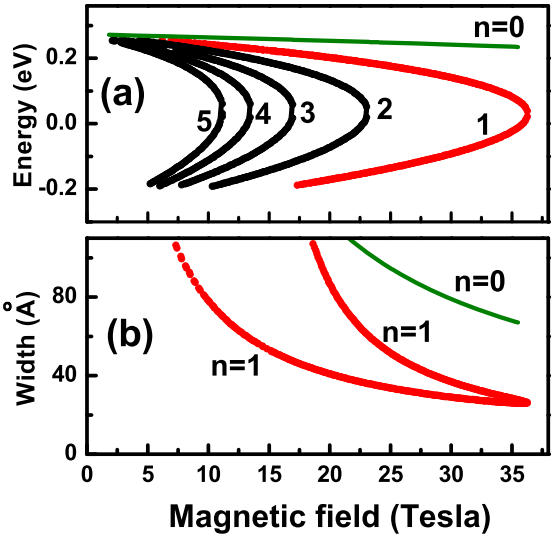

Fig. 3: (Colour on-line) (a) The LL energy spectrum of an electron in a junction between two TIs is shown as a function of the magnetic field for a few lowest LLs. The numbers next to the lines are the LL indices. The TIs have the same Hamiltonian parameters, except for A_1, $A_1 = 2.2\,\text{eV}\cdot\text{Å}$ for TI-1 and $A_1 = 4.0$ eV·Å for TI-2. (b) The width in the z-direction of the LL wave functions is shown for $n = 0$ and $n = 1$ LLs.

momentum m,

$$V_m^{(n)} = \int_0^\infty \frac{\mathrm{d}q}{2\pi} qV(q)\left[F_n(q)\right]^2 L_m(q^2)e^{-q^2}. \qquad (5)$$

Here $L_m(x)$ are the Laguerre polynomials, $V(q) = 2\pi e^2/(\kappa\ell_0 q)$ is the Coulomb interaction in the momentum space, κ is the dielectric constant, $\ell_0 = \sqrt{e\hbar/cB}$ is the magnetic length, and $F_n(q)$ is the form factor for the n-th Landau level. The form factors for tachyons are

$$F_{n=0}(q) = L_0\left(\tfrac{1}{2}q^2\right), \qquad (6)$$

$$F_{n\geqslant 1}(q) = \cos^2\alpha_n L_n\left(\tfrac{1}{2}q^2\right) + \sin^2\alpha_n L_{n-1}\left(\tfrac{1}{2}q^2\right). \qquad (7)$$

The form factor of the $n = 0$ LL (eq. (6)) is identical to that of graphene and also to that of the non-relativistic systems. However, for $n \geqslant 1$ the form factor of the tachyon system becomes unique. For graphene and for the non-relativistic systems, the corresponding form factors are $F_n^{(\mathrm{NR})} = L_n$ and $F_n^{(\mathrm{Gr})} = \frac{1}{2}(L_n + L_{n-1})$, respectively. In both cases the form factors are independent of the magnetic field. For tachyons, on the other hand, the form factor (7) depends on the magnetic field through the effective angle $\alpha_n(B)$. With increasing magnetic field the tachyon form factor, $F_{n\geqslant 1}$, changes from the non-relativistic value, $F_n^{(\mathrm{NR})}$ (point B in fig. 2(a)) or $F_{n-1}^{(\mathrm{NR})}$ (point A in fig. 2(a)), in a small magnetic field, $B \to 0$, to the form factor of graphene [13], for $B = B^*$.

The FQHE with an incompressible ground state can be observed only in the LL with strong short-range repulsion, *i.e.*, a fast decay of the corresponding pseudopotentials, V_m, with m. Such a strong repulsion is realized only in the LL with a strong admixture of $\phi_{0,m}$. Therefore, in a tachyonic system the FQHE is expected only in the $n = 0$ and $n = 1$ LLs. To study the strength of the corresponding FQHE we numerically evaluate the energy spectrum of a finite N-electron system in a spherical geometry [12] with the radius of the sphere $\sqrt{S}\ell_0$. Here $2S$ is the integer number of magnetic fluxes through the sphere in units of the flux quantum. This determines the filling factor ν of the system. For example, $\nu = 1/q$ (q is an odd integer) corresponds to $S = (\frac{q}{2})(N-1)$ [11].

In fig. 2(b) the energy gap for $\nu = \frac{1}{3}$ is shown for $n = 0$ and $n = 1$ LLs of the tachyonic system [14]. For the $n = 0$ LL, the gap does not depend on B and is exactly equal to the gap for the $n = 0$ non-relativistic LL. This is because the $n = 0$ tachyonic LL wave function consists of only $\phi_{0,m}$. For the $n = 1$ LL, however, the wave function is the B-dependent mixture of $\phi_{0,m}$ and $\phi_{1,m}$. As a result the gap depends on the magnetic field and changes from the $n = 0$ non-relativistic LL value for $B \to 0$ (point A) to the $n = 1$ graphene LL value for $B = B^*$ (point G) and finally to $n = 1$ non-relativistic LL value at point B (in the thermodynamic limit such a state becomes compressible).

The maximum gap in a non-relativistic system corresponds to the green line in fig. 2(b), while the maximum gap in graphene corresponds to point G in fig. 2(b). Therefore, comparing the data in fig. 2(b), we conclude that within some range of the magnetic fields (which is shown in fig. 2(b) by an oval curve), the gap in our model tachyon system is the largest compared to all other available 2D systems. The tachyon dispersion relation provides an unique possibility to study, within a single tachyonic $n = 1$ LL, the properties of the $n = 0$ non-relativistic LL (point A in fig. 2(a)), $n = 1$ graphene LL (point G in fig. 2(a)), and $n = 1$ non-relativistic LL (point B in fig. 2(a)).

Three-dimensional (3D) model for the junction states between two TIs: Until now, we have discussed the magnetic-field effects via an effective Hamiltonian for tachyons. The tachyonic dispersion can be realized also in the junction of two TIs [3]. The junction dispersion relation in this case is approximately described by the effective Hamiltonian (1). The realization of the tachyonic excitations as the junction states bring additional factors into consideration. For example, the junction states have a finite width in the z-direction which can reduce the interaction strength in that system.

We consider the junction at $z = 0$ between two TI insulators: TI-1 for $z < 0$ and TI-2 for $z > 0$. The electronic properties of both TIs are described by the same type of low-energy effective 3D Hamiltonian [9,15] of the matrix form

$$\mathcal{H}_{\mathrm{TI}} = \epsilon(\vec{p}) + \begin{pmatrix} M(\vec{p})\sigma_z - \mathrm{i}A_1\sigma_x\partial_z & (A_2/\hbar)p_-\sigma_x \\ (A_2/\hbar)p_+\sigma_x & M(\vec{p})\sigma_z + \mathrm{i}A_1\sigma_x\partial_z \end{pmatrix}, \qquad (8)$$

where $\partial_z = \partial/\partial z$, and

$$\epsilon(\vec{p}) = C_1 - D_1\partial_z^2 + (D_2/\hbar^2)(p_x^2 + p_y^2), \tag{9}$$

$$M(\vec{p}) = M_0 + B_1\partial_z^2 - (B_2/\hbar^2)(p_x^2 + p_y^2). \tag{10}$$

We assume that for both TIs, all parameters in eq. (8) are the same as for Bi_2Se_3, except A_1 which is 2.2 eV for TI-1 and 4.0 eV for TI-2. For these parameters, the junction states exhibit the tachyonic dispersion [3]. The four-component wave function corresponding to (8) determines the amplitudes of the wave functions at the positions of Bi and Se atoms: ($Bi_\uparrow$, $Se_\uparrow$, $Bi_\downarrow$, $Se_\downarrow$), where the arrows indicate the direction of the electron spin.

The Hamiltonian of the TI in an external magnetic field, pointing along the z-direction, can be obtained from (8) by replacing the 2D momentum (p_x, p_y) with the generalized momentum (π_x, π_y) [16] and introducing the Zeeman energy, $\Delta_z = \frac{1}{2}g_s\mu_B B$. For the Hamiltonian (8) in a magnetic field, the wave function in the n-th LL has the general form

$$\Psi^{(\mathrm{TI})}_{n\geqslant 1}(z) = \begin{pmatrix} \chi_1^{(n)}(z)\phi_{n-1,m} \\ \chi_2^{(n)}(z)\phi_{n-1,m} \\ \chi_3^{(n)}(z)\phi_{n,m} \\ \chi_4^{(n)}(z)\phi_{n,m} \end{pmatrix}. \tag{11}$$

Therefore, the wave function $\Psi^{(\mathrm{TI})}_{n\geqslant 1}$ is again a mixture of n and $n-1$ non-relativistic LL functions. For the $n=0$ LL, only $\chi_1^{(n=0)}$ and $\chi_2^{(n=0)}$ are zero.

To find the LL junction states, we follow the same procedure as for the LL surface states of a TI [3,16–18]. For each TI we find the general bulk solution of the Schrödinger equation in the form of $\Psi \propto e^{\lambda^{(m)}z}$, where $\lambda^{(m)}$ is a complex constant, and $m=1$ and 2 for TI-1 and TI-2, respectively. This solution has a given energy, E, and a given LL index, n. The corresponding $\lambda^{(m)}$ are determined from a secular equation, $\det[\mathcal{H}_{TI}^{(m)}(\vec{k}, \lambda^{(m)}) - E] = 0$, for each TI. For each energy E and the LL index n, the secular equation provides eight values of $\lambda_j^{(m)}(n, E)$, $j = 1, \ldots, 8$ with the corresponding wave functions. Second, since we are searching for the localized LL junction states, we need to choose (for each TI) only four values of $\lambda_j^{(m)}$ out of eight with the properties: $\mathrm{Re}\lambda_j^{(m)} > 0$ for TI-1 ($z<0$) and $\mathrm{Re}\lambda_j^{(m)} < 0$ for TI-2 ($z>0$). We then choose the corresponding four wave functions (for each TI) as the basis and expand the solution for the LL junction state in this basis. Finally, the energy of the LL junction state is found from the condition of continuity of the wave function, $\Psi_n^{(\mathrm{TI})}(z)$, and the current $[\delta\mathcal{H}_{\mathrm{TI}}/\delta k_z]\Psi_n^{(\mathrm{TI})}$ in the junction.

The spectrum of the LL junction states corresponding to the tachyonic dispersion is shown in fig. 3(a). The spectrum is qualitatively similar to that (see fig. 2(a)) obtained from the model 2D Hamiltonian. In both cases, the LLs exist only for a limited range of magnetic fields and energies. In weak magnetic fields, the LL spectra of the junction states and for the 2D model are different. For a given LL index n, there are no junction states for weak magnetic fields. These junction states are delocalized in the z-direction. To illustrate this delocalization we show in fig. 3(b) the width of the $n=0$ and $n=1$ LL wave functions in the z-direction. At a singular point of the LL spectrum, *i.e.*, for $B = B^*$, where the derivative of the LL energy with respect to the magnetic field becomes infinitely large, the LL wave functions have the smallest width. This width increases with decreasing magnetic field and finally the LL junction states are delocalized in the z-direction. A similar behavior is observed for $n=0$ LL, but there is no singular point in this case. Therefore, the LL energy spectrum of the junction states in the regime of tachyonic dispersion can be well described by the 2D effective model near the singular point $B \sim B^*$.

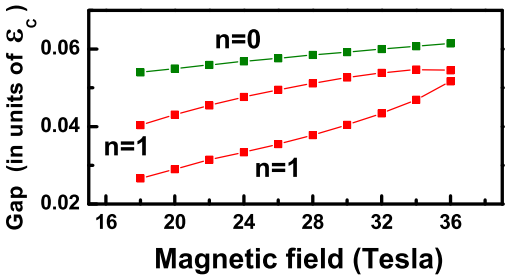

Fig. 4: (Colour on-line) The energy gap at $\nu = \frac{1}{3}$ for $n=0$ (green line) and $n=1$ (red line) LLs in the junction of two TIs. The corresponding LLs are shown in fig. 3(a) by green and red lines, respectively. The gap is calculated for a finite-size system with $N=9$ particles in a spherical geometry with $S=12$. The gap is given in units of the Coulomb energy, $\epsilon_{\mathrm{C}} = e^2/\kappa\ell_0$.

As long as the finite size of the localized modes, *i.e.*, the spatial width of the mode in the z-direction, does not introduce additional dynamics in the z-direction, these modes are the 2D junction states. The dynamics in the z-direction is introduced, for example, through scattering by impurities or by additional boundaries of TIs. In this case the surface junction states are mixed with the bulk states, which results in broadening of the junction states, and they cannot be identified as the states localized at a junction.

We have evaluated the gaps for the $n=0$ and $n=1$ junction LLs. We have used the same approach as for the 2D model of the tachyonic excitations, discussed above. The results are shown in fig. 4. Quantitatively the behavior of the gap as a function of the magnetic field is similar to that of the 2D model of the tachyonic excitations (fig. 2(b)). Due to a finite width of the LL wave functions in the TI junction, there is a reduction of the inter-electron interaction strength and correspondingly the gap. This reduction is visible for $n=0$ LL, where a smaller gap and the magnetic-field dependence of the gap is shown in fig. 4.

Although for the 2D tachyon model the gap is the largest for the $n=1$ LL, for the junction LLs the gap is the largest for the $n=0$ LL, due to the non-zero spin polarization of the $n=1$ junction LL. This spin polarization is clearly visible from the general property of the LL wave function (eq. (11)); only the components $\chi_3^{(n=0)}$ and $\chi_4^{(n=0)}$ of $\Psi_{n=0}^{(\mathrm{TI})}$ are non-zero and these components correspond to the spin-down polarization. The numerically found $n=1$ LL wave functions also show partial spin-down polarization. As a result, the LL wave function have larger contribution from the $\phi_{n=1}$ non-relativistic LL function, which reduces the inter-electron interaction strength and also the gap. The spin polarizations of the surface states and corresponding spin symmetry breaking occur even for the surface states of isolated TI (within the effective approach the surface states are described by effective relativistic massless Dirac Hamiltonian). Such surface states have spin chiral nature without double spin degeneracy. This is different from graphene, which has chiral nature in terms of pseudospin and still have double spin degeneracy. In a TI, the chiral nature of the states and lifting of spin degeneracy occurs due to strong spin-orbit interactions.

The energies of the surface states in a junction between two TIs lie in the bulk band gap of both TIs. The coupling of the junction states to the bulk TI states is introduced through irregularities in TIs, such as impurities or defects in the bulk of TIs. Such a coupling results in broadening and finite lifetime of the junction states. For strong coupling the broadening becomes so strong that the junction states cannot be defined. Therefore the well-defined junction states can be introduced only for weak coupling between the surface and the bulk states. The coupling is weak for a small spatial extension of the junction states in the z-direction and for large bulk band gap of TIs. Therefore, to observe the junction states one needs to employ the TIs with large bulk band gaps and consider well-localized, *i.e.*, with small spatial extension, junction states. Among all the TIs that are realized experimentally at present, the Ti_2Se_3 has the largest bulk band gap of 0.3 eV. But even for Ti_2Se_3 there are many defect states in the bulk, which results in electron transport through TI not through the gapless surface states but through the gapped bulk of the material. To observe the junction states by the transport measurements, the quality of TIs need to be improved. Another requirement on the properties of two TIs is that the parameters of TIs should be quite different. This difference can be introduced even for a single TI, where the junction states are realized at the boundary between two regions with different orientations of the crystallographic axes. The possibility of realization of tachyonic dispersion in this case requires additional analysis. To probe the specific features of tachyonic LLs the magnetic field should be relatively large and up to 30 T (see figs. 3 and 4).

In addition to unique properties of the LL spectrum of tachyonic excitations, the tachyons can be also detected in the transport measurements. If the transport through the junction surface states can be realized experimentally, then such transport, for example, in time resolved experiments, should reveal the specific tachyonic dispersion relation.

To summarize: we have investigated the magnetic-field effects of tachyons along the interface of two topological insulators. We used an effective two-dimensional model Hamiltonian for tachyons and the three-dimensional model for the junction states of the two TIs, both developed by us in ref. [3]. The Landau levels in both these models show very similar behavior. Unlike in graphene or in conventional electron systems, only a few LLs are found to exist for tachyons. Only one LL ($n=0$) survives in large magnetic fields. The $\nu=\frac{1}{3}$ FQHE state is the strongest (within a limited range of the magnetic field) when compared with that for conventional 2D electron systems and in graphene. Interestingly, the FQHE in the $n=1$ LLs for tachyons describes the FQHE of the $n=0,1$ LLs of the non-relativistic electron system and that of the $n=1$ graphene LL in different regions of the magnetic field. Experimental confirmation of these unique properties of the Landau levels would provide very strong evidence for the existence of elusive tachyons.

* * *

The work has been supported by the Canada Research Chairs Program of the Government of Canada.

REFERENCES

[1] Hasan M. Z. and Kane C. L., *Rev. Mod. Phys.*, **82** (2010) 3045; Qi X.-L. and Zhang S.-C., *Rev. Mod. Phys.*, **83** (2011) 1057.

[2] Abergel D. S. L., Apalkov V., Berashevich J., Ziegler K. and Chakraborty T., *Adv. Phys.*, **59** (2010) 261.

[3] Apalkov V. and Chakraborty T., *EPL*, **100** (2012) 17002.

[4] Bilaniuk O. M. P., Deshpande V. K. and Sudarshan E. C. G., *Am. J. Phys.*, **30** (1962) 718; Bilaniuk O. M. and Sudarshan E. C. G., *Phys. Today*, **22**, issue No. 5 (1969) 43; Feinberg G., *Phys. Rev.*, **159** (1967) 1089; Newton R. G., *Phys. Rev.*, **162** (1967) 1274; Recami E., *J. Phys.: Conf. Ser.*, **196** (2009) 012020; *Found. Phys.*, **31** (2001) 1119; Jentschura U. D. and Wundt B. J., *J. Phys. A: Math. Theor.*, **45** (2012) 444017.

[5] Chiao R. Y., Kozhekin A. E. and Kurizki G., *Phys. Rev. Lett.*, **77** (1996) 1254.

[6] Mugnai D., Ranfagni A. and Ruggeri R., *Phys. Rev. Lett.*, **84** (2000) 4830.

[7] Takahashi R. and Murakami S., *Phys. Rev. Lett.*, **107** (2011) 166805.

[8] Chodos A., Hauser A. I. and Kostelecky V. A., *Phys. Lett. B*, **150** (1985) 431; Ehrlich R., *Am. J. Phys.*, **71** (2003) 1109.

[9] Liu C.-X., Qi X.-L., Zhang H. J., Dai X., Fang Z. and Zhang S.-C., *Phys. Rev. B*, **82** (2010) 045122.
[10] Wang Z., Fu Z.-G., Wang S.-Xi and Zhang P., *Phys. Rev. B*, **82** (2010) 085429.
[11] Chakraborty T. and Pietiläinen P., *The Quantum Hall Effects*, 2nd edition (Springer, New York) 1995.
[12] Haldane F. D. M., *Phys. Rev. Lett.*, **51** (1983) 605.
[13] Apalkov V. M. and Chakraborty T., *Phys. Rev. Lett.*, **97** (2006) 126801.
[14] The FQHE gap for a single TI is reported in Apalkov V. M. and Chakraborty T., *Phys. Rev. Lett.*, **107** (2011) 186801.
[15] Zhang H., Liu C.-X., Qi X.-L., Dai Xi, Fang Z. and Zhang S.-C., *Nat. Phys.*, **5** (2009) 438.
[16] Yang Z. and Han J. H., *Phys. Rev. B*, **83** (2011) 045415.
[17] Zhou B., Lu H. Z., Chu R. L., Shen S. Q. and Niu Q., *Phys. Rev. Lett.*, **101** (2008) 246807.
[18] Shan W.-Y., Lu H.-Z. and Shen S.-Q., *New J. Phys.*, **12** (2010) 043048.